INSTITUTE OF PHYSICS PUBLISHING JOURNAL OF OPTICS B: QUANTUM AND SEMICLASSICAL OPTICS
J. Opt. B: Quantum Semiclass. Opt. **6** (2004) S169–S176 PII: S1464-4266(04)72481-7

REVIEW ARTICLE

Localized structures and their dynamics in a liquid crystal light valve with optical feedback

S Residori[1,5], A Petrossian[2], T Nagaya[3] and M Clerc[4]

[1] Institut Non-Linéaire de Nice, UMR 6618 CNRS-UNSA, 1361 Route des Lucioles, 06560 Valbonne, France
[2] Laboratoire de Physique de l'ENS-Lyon, 46 Allée d'Italie, 69364 Lyon, France
[3] Department of Electrical and Electronic Engineering, Faculty of Engineering, Okayama University, Okayama 700-8530, Japan
[4] Departamento de Física, Facultad de Ciencias Físicas y Matemáticas, Universidad de Chile, Casilla 487-3, Santiago, Chile

Received 18 November 2003, accepted for publication 4 March 2004
Published 4 May 2004
Online at stacks.iop.org/JOptB/6/S169
DOI: 10.1088/1464-4266/6/5/002

Abstract
In this article we review the conditions for the appearance of localized states in a nonlinear optical system, with particular reference to the liquid crystal light valve (LCLV) experiment. The localized structures here described are of dissipative type; that is, they represent the localized solutions of a pattern-forming system. We discuss their features of stable addressable localized states, and we show that they dispose themselves on the nodes of highly symmetric lattices, as obtained by the introduction of an N-order rotation angle in the optical feedback loop. The stability is lost either on increase of the input light intensity or by the introduction of an extra small angle of rotation. The complex spatio-temporal dynamics that follows is characterized by oscillations in the position of the localized states. We discuss the origin of this permanent dynamics in relation to the non-variational character of the LCLV system, underlining the general character of such complex behaviours of localized states.

Keywords: nematic liquid crystals, localized structures, spatiotemporal phenomena

1. Introduction

Non equilibrium processes often lead in nature to the formation of spatially periodic and extended structures, so-called patterns [1]. The birth of a pattern from a homogeneous state takes place through the spontaneous breaking of one or more of the symmetries characterizing the system [2]. In some cases, it is possible to localize a pattern in a particular region of the available space, so that we deal with localized instead of extended structures. From a theoretical point of view, localized structures in out of equilibrium systems can be seen as a sort of dissipative solitons [3]. Experimentally, during the last few years localized patterns or isolated states have been observed in many different fields. Examples are domains in magnetic materials [4], chiral bubbles in liquid crystals [5], current filaments in gas discharge experiments [6], spots in chemical reactions [7], oscillons in granular media [9], localized fluid states in surface waves [8] and in thermal convection [10], and solitary waves in nonlinear optics [11–18]. All these localized states can be considered to belong to the same general class of localized structures; that is, they are patterns that extend only over a small portion of a spatially extended system. The mechanisms of localization of spatial structures rely on

[5] Author to whom any correspondence should be addressed.

two main ingredients: the bistability, either between two homogeneous states or between a homogeneous state and a spatially periodic one, and the existence of an intrinsic spatial length, which is necessary to stabilize a localized state and which determines its typical size [19].

In optics, solitary waves were first predicted to appear in bistable ring cavities [11]. Then, localized states have been largely studied not only for their fundamental properties but also in view of their potential applications in photonics [20–23]. Sometimes named as cavity solitons, optical localized structures have been observed in photorefractives [24], in lasers with a saturable absorber [25], in liquid crystal light valves (LCLVs) with optical feedback [12–16], in Na vapours [26], and more recently in semiconductor micro-cavities [18].

In order to take advantage of localized structures for photonics applications, it appears essential to understand the conditions for their stable localization as well as their intrinsic dynamical behaviour. Most of the theoretical models proposed up to now, for example in optics [27] and in chemistry [28], consider localized structures as the stationary solutions of a corresponding variational system whose dynamics is characterized by the minimization of a Lyapunov functional. The associated dynamics is a transient relaxation to the global minimum, corresponding to the most stable stationary state. Nevertheless, localized structures may in general appear in a system that are of non-variational type [3]. As a consequence, it is generically expected that localized structures show permanent dynamics, such as propagation and oscillations of their positions [29], in analogy with other non-variational effects such as phase turbulence [30], propagation of Ising–Bloch walls, predicted in oscillatory media [31] and observed in liquid crystal experiments [32], and rotation of spirals in excitable media [33].

In this article we review the conditions for the appearance of localized states in a nonlinear optical system, with particular reference to the liquid crystal light valve experiment. In this system the bistability between homogenous states results from the subcritical character of the Fréedericksz transition, when the local electric field, which applies to the liquid crystals, depends on the liquid crystal reorientation angle [35, 36]. In the optical feedback loop, the bistability is present together with a pattern forming diffraction length. This assures the presence of the two necessary ingredients, bistability and a critical length scale, for the appearance of localized structures [12–15].

Here, we present the features of stable localized structures as single addressable elements, disposing themselves on the nodes of highly symmetric lattices, as obtained by the introduction of an N-order rotation angle in the feedback loop. As we have recently shown, the stability is lost either on increase of the input light intensity or by the introduction of an extra small angle of rotation [16], and the complex spatio-temporal dynamics that follows is characterized by oscillations in the position of the localized states. Recently, we have proposed that the origin of the permanent dynamics is related to the non-variational character of the LCLV system [34]. New results are presented in this paper, showing that the N-order configurations of localized structures becomes unstable for a slight increase of the input pump intensity.

The article is divided as follows. The experiment is presented in section 2, and in section 3 we show ordered and symmetric configurations of localized structures observed in the presence of an N-order rotation feedback. In section 4, we present a mechanism of structure destabilization through the introduction of a non-local shift in the optical feedback loop [16]. Section 5 contains new results on the intrinsic and permanent dynamics that characterize the localized structures for increasing input light intensity. In section 6 we present a theoretical model that we have recently derived and that leads to a Lifshitz normal form equation [34]. Section 7 is the conclusions.

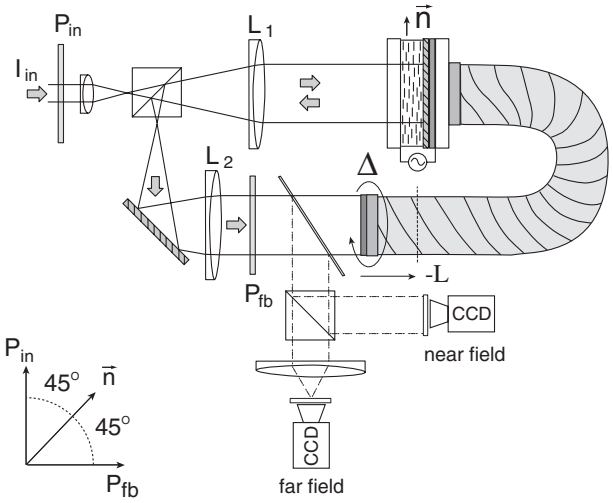

Figure 1. The experimental set-up: the LCLV is illuminated by a plane wave; the wave, reflected by the dielectric mirror inside the LCLV, is sent back to the photoconductor through the optical fibre bundle. Δ is the angle of rotation of the fibre with respect to the front side of the LCLV. $\vec{n}$ is the liquid crystal nematic director; $P_{\rm in}$ and $P_{\rm fb}$ are the input and feedback polarizers; L_1 and L_2 are two confocal 25 cm focal length lenses. $-L$ is the free propagation length, negative with respect to the plane on which a 1:1 image of the front side of the LCLV is formed.

2. Description of the experiment

The experiment, shown in figure 1, consists of an LCLV with optical feedback, as it was originally designed by the Akhmanov group [37]. The LCLV is composed of a nematic liquid crystal film sandwiched between a glass window and a photoconductive plate over which a dielectric mirror is deposited. The coating of the bounding surfaces induces a planar anchoring of the liquid crystal film (nematic director $\vec{n}$ parallel to the walls). Transparent electrodes covering the two confining plates permit the application of an electric field across the liquid-crystal layer. The photoconductor behaves like a variable resistance, which decreases with increasing illumination. The feedback is obtained in the following way: the light which has passed through the liquid-crystal layer, and has been reflected by the dielectric mirror inside the LCLV, is sent back onto the photoconductor of the LCLV. This way, the light beam experiences a phase shift which depends on the liquid crystal reorientation and, in its turn, modulates the effective voltage that locally is applied to the liquid crystals. Thus, a feedback is established between the liquid crystal reorientation and the local electric field.

The feedback loop is closed by an optical fibre bundle and is designed in such a way that diffraction and polarization

interference are simultaneously present [12]. The free end of the fibre bundle is mounted on a precision rotation stage, which allows us to fix a feedback rotation angle Δ with a precision of $\pm 0.01°$. The optical free propagation length is fixed to $L = -10$ cm. At the linear stage for the pattern formation, a negative propagation distance selects the first unstable branch of the marginal stability curve, as for a focusing medium [38]. The angles that the input and feedback polarizers form with the liquid crystal director are fixed to 45° and −45°, respectively. For this parameter setting and close to the point of the Fréedericksz transition, there is coexistence between a periodic pattern and a homogeneous solution. The Fréedericksz transition point is attained for an applied voltage V_0 of approximately 3 V_{rms} with a frequency of 5 kHz [35].

By increasing V_0, successive branches of bistability are excited. Most of the experimental observations here reported were obtained close to the bistable branch located around $V_0 = 18.5$ V_{rms}. For this high value of the applied voltage, the reoriented liquid crystal sample becomes similar to a homeotropic one (nematic director $\vec{n}$ perpendicular to the confining walls), the light feedback inducing only a small reorientation around its equilibrium state. The bistable behaviour here observed is similar to the one observed close to the Fréedericksz transition point: the LCLV works closely around a branch of bistability, where it may be assimilated to a phase slice with a step-like response [34]. But, because of the high V_0, the nematic director being almost aligned with the applied electric field and the LCLV being close to the saturation of its response, the system becomes much less sensitive to external perturbations coming from noise sources or spatial inhomogeneities.

The total incident intensity is $I_{in} = 0.90$ mW cm^{-2}. A 50% beam splitter is positioned before the LCLV, so that the intensity of the feedback light beam is limited to 25% of the total incoming intensity. This condition ensures that the LCLV works only around the switch-up point of this bistable response. The input beam has a Gaussian profile with a transverse size of approximately 2 cm, whereas a diaphragm before the fibre bundle selects a central active zone with a diameter of 1.2 cm.

3. Crystal-like symmetries of localized structures

Here we review the typical distributions of localized structures that are observed close to a point of nascent bistability. In the parameter space, the points of nascent bistability are identified as the locations where the surface of stationary states becomes s-shaped. The control parameters of the experiments are the applied voltage, V_0, and the input light intensity, I_{in}. For this set of experiments the parameters are fixed to $V_0 = 18.45$ V_{rms} at 5 kHz frequency and $I_{in} = 0.90$ mW cm^{-2}. The feedback rotation angle is $\Delta = 2\pi/N$, with N integer, and constitutes a geometrical constraint imposing an overall N-order symmetry to the system.

The size of each localized structure is approximately $\Lambda = 350$ μm, which corresponds to the basic wavelength $\Lambda = 2\pi/q_0 = \sqrt{2\lambda L}$ ($\lambda = 632$ nm is the optical wavelength) predicted by linear analysis for a focusing medium with a feedback mirror [41]. The distance between the spots is in average much larger than their individual size, which indicates that we are dealing with a collection of localized structures instead of a fully correlated pattern. Here, for a fully correlated pattern we mean an extended texture that fully covers a large portion of the space and that cannot be decomposed into its basic constituent cells.

Depending on the initial conditions and on the value of $\Delta = 2\pi/N$, different stationary configurations of localized structures may be obtained. By choosing different N we can construct highly regular distributions of light spots, that, once they have appeared, remain fixed to their positions. If we perturb the system by blocking the feedback loop, another configuration may appear. Actually, since the system is close to a point of nascent bistability, the dark homogeneous state is also stable. Thus, once they are erased by blocking the feedback loop, there are no localized structures until we introduce a perturbation able to trigger their appearance. This can be done either by slightly, and temporarily, increasing V_0, or by injecting in the feedback loop a weak additional light beam, such as that of a commercial laser pointer. By means of this local writing procedure we can trigger the appearance of light spots at specific local sites, corresponding to the structure function of an N-order crystal. This allows us to construct in real space a sort of 'crystallography', where all the N rotational-order structures may be figured out. A few examples are displayed in figure 2, where we show the crystal and quasicrystal-like distributions of light spots that are observed for $\Delta = 2\pi N$ with $N = 2, 3, 4, 5, 6, 7, 8, 9$.

With the laser pointer, it is possible to address different positions for the appearance of localized structures. Starting from a single set of N localized structures, we can locally perturb the system and switch on another set in a different position or a single spot in the centre. These manipulations prove that the observed spots are indeed localized structures, in the sense that the whole pattern is highly decomposable; that is, each structure may be considered as a single element, independent of the other structures [39]. More precisely, for the N-order symmetry imposed by the rotation angle, the basic independent element that we have to consider is a set of N structures, always appearing along concentric rings. The centre is a singular point, that may or not be occupied by a single spot, depending on the initial conditions.

Note that, since a configuration of localized structures is completely decomposable, an infinite number of possible combinations may be obtained for each value of N. Thus, the pictures displayed in figure 2 are just examples to elucidate the mechanism for the construction of a 'crystal-like' pattern. No quantitative prediction can be made on such a kind of pattern, except the evaluation of the maximum information that can be stored. In other words, the quantity that would be required to identify a configuration of localized structures would be a kind of spatial entropy, for which a clear definition is still lacking. Practical applications, like information storage and retrieval, are related to the decomposable nature of these patterns and, in fact, a first successful demonstration has recently been reported [40].

The localization in the near-field manifests its counterpart as a strong delocalization in the far-field. Indeed, observations in the far-field show a diffusion of the light intensity around the central peak (zero spatial frequency). At the same time, no wavevector structure is distinguishable. A typical far-field

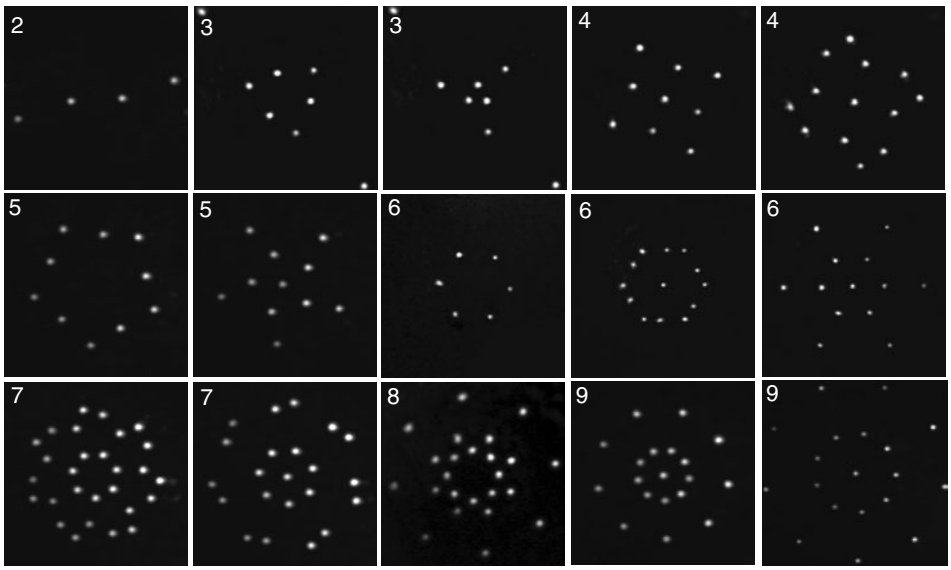

Figure 2. Examples of near-field images of stationary localized structures for $\Delta = 2\pi/N$ with $N = 2, 3, 4, 5, 6, 7, 8, 9$, as labelled in each frame. In the $N = 9$ right-hand bottom frame, the magnification factor is $2/3$ with respect to the other pictures.

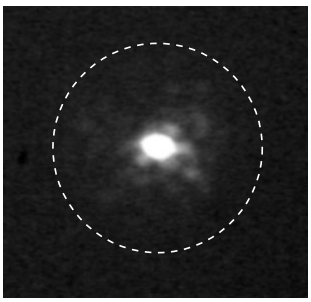

Figure 3. A typical image observed in the far-field for all the values of N.

image is displayed in figure 3, where the dashed line marks the location that would be occupied by the wavevectors of a fully correlated pattern, at the spatial frequency $q_0 = 2\pi/\Lambda$, corresponding to the size of the individual spots. The same diffraction pattern is observed in the far-field for all the values of N. On the other hand, the near-field N-order spot distributions look like the spectral counterpart (far-field) of the spatially extended crystals and quasi-crystals that appear in an LCLV experiment with diffractive feedback [42].

4. Ring dynamics induced by a non-local shift in the feedback loop

As we have recently shown [16], if we introduce a small additional rotation angle, $\delta = 0.1°$, in such a way that $\Delta = 2\pi/N + \delta$, the localized structures acquire a rotation dynamics along concentric rings. Even though the non-local shift, δ, is along one direction, often, two adjacent rings rotate in opposite directions. Instantaneous snapshots of the dynamical rings are shown in figure 4 for $N = 3, 4, 6$. Note that similar near-field patterns, *Akhseals*, have also been reported by the Akhmanov group [37]. Even though they are not explained in terms of localized structures, they are indeed observed in experimental conditions similar to ours.

For $\Delta = 2\pi/N + \delta$ and $\delta = 0.1°$, we have set the applied voltage to $V_0 = 18.49$ V_{rms} (5 kHz). For this value of V_0, the structures appear spontaneously, nucleating from the intrinsic noise in the LCLV (inhomogeneities or fluctuations). Moreover, the slight gradients provided by the Gaussian beam profile impose O(2) circular symmetry, leading to the appearance of successive and concentric rings. Other shapes of the beam profile or different initial conditions would lead to different distributions of localized structures, as shown numerically in [43].

After their appearance, the spots rotate over the rings whereas the ring diameter changes with time. Eventually, the radial motion may lead to the collapse of two adjacent rings or to the splitting of one ring into two neighbouring ones. Each ring reflects the underlying symmetry, so that the number of spots is N on the inner ring and increases by steps of N over two adjacent ones. However, for the outer rings, the number of spots becomes 'wrong'; that is, either one spot is missing with respect to the underlying N-order symmetry or there is an extra spot.

In figure 5, azimuthal and radial spatio-temporal plots are reported as an example of the rings dynamics. The azimuthal (θ–t) spatio-temporal plots displayed in figures 5(a) and (b) show the rotation of the localized structures over the 12 and 17 spot rings, that are counter-rotating with different speed of rotation. At longer times, eventually each ring undergoes a radial instability, leading to the creation and annihilation of adjacent rings. An example is shown in (c), where the fusion of two adjacent spots leads to the transition from 12 to 6 localized structures. In the azimuthal plots the radial distance is normalized to the instantaneous diameter of each ring. In (d) we show a radial (r–t) spatio-temporal plot (averaged over θ), where the ring creation–annihilation may be distinguished.

We show in figure 6 the measured speed of rotation v_n for increasing number n of spots along the successive rings. It must be recalled that the diameter of the rings is not constant with time, so that the number n is only roughly related to the distance from the centre. The measured data suggest that the

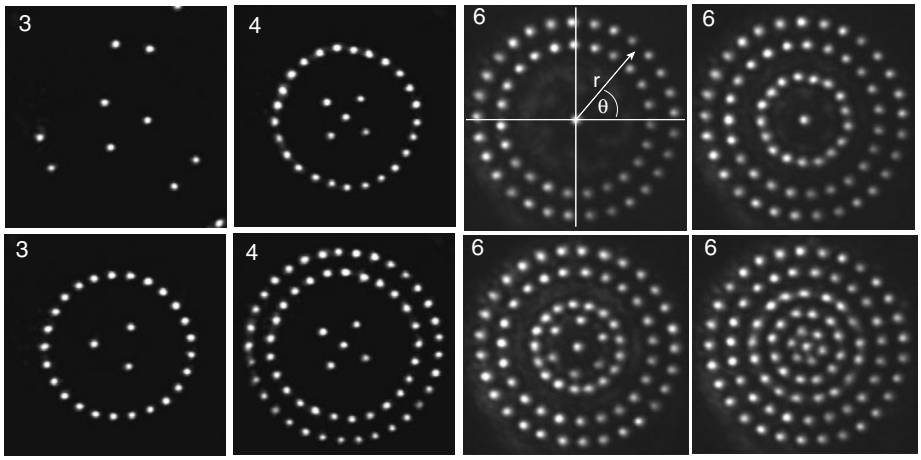

Figure 4. The localized structures acquire a rotation dynamics when $\Delta = 2\pi/N + 0.1^\circ$ with $N = 3, 4, 6$, as labelled in each frame.

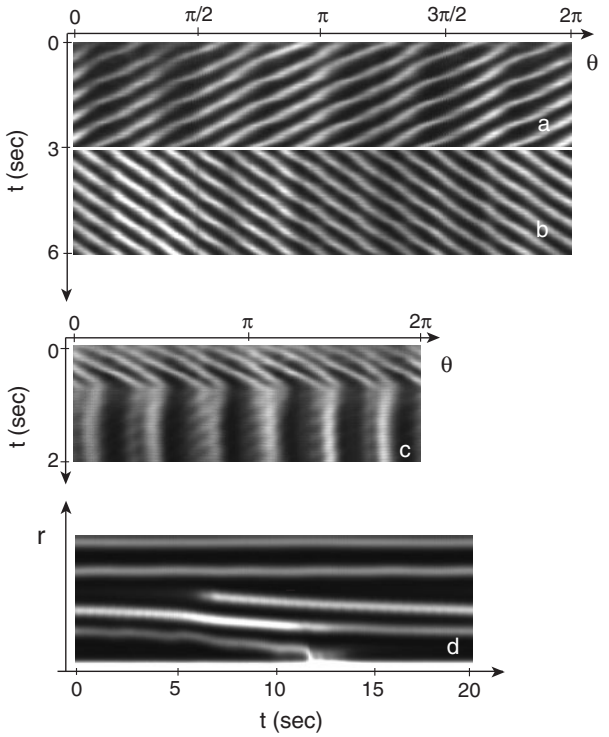

Figure 5. Azimuthal (θ–t) space–time plots for (a) a 12-spot and (b) a 17-spot ring; (c) shows the transition from 12 to 6 spots. (d) A radial (r–t) space–time plot showing the creation and annihilation of rings.

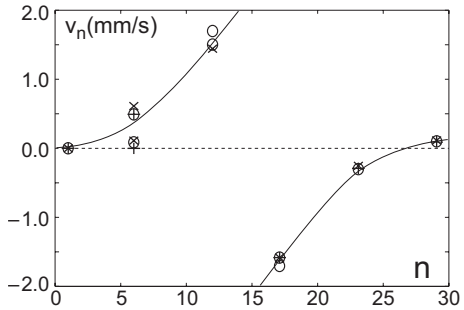

Figure 6. The speed of rotation for increasing number n of localized structures along successive rings.

change of rotation direction could be related to the existence of a critical radius, above which an overall phase shift changes its sign. Correspondingly, the number of spots along the outer rings becomes 'wrong'.

5. Intrinsic dynamics of localized structures

5.1. Two-dimensional and rotated case

As a consequence of the non-variational character of the LCLV experiment, we expect that localized structures exhibit an intrinsic and permanent dynamics for some range of the control parameters. Indeed, as we show here, when the input light intensity is slightly increased above the point of nascent bistability, we observe oscillations in the positions of the localized structures, and this even though the feedback rotation angle Δ is exactly fixed to a value commensurate to 2π. In figure 7 we show instantaneous snapshots of the $N = 5$ distributions observed in the same experimental conditions as for figure 2 but for a larger value of the input light intensity, $I_{\text{in}} = 0.95$ mW cm^{-2}. The observed dynamics consists of a periodic bouncing of two adjacent spots one over the other.

The periodic behaviour can be extracted by drawing a spatio-temporal plot along a line passing through the centres of two adjacent spots, as shown by the dashed line in figure 7(a). The resulting diagram is displayed in figure 8. On further increasing I_{in}, the oscillations in the structure positions become irregular in time. Similar dynamical behaviour can be observed for all N-order distributions of localized structures.

5.2. One-dimensional and non-rotated case

In order to single out the dynamics independently of the symmetry imposed by the feedback rotation angle Δ, we have carried out one-dimensional experiments by fixing $\Delta = 0^\circ$ [34]. In this case, the system becomes very sensitive to the influence of optical misalignments, such as small drifts, inhomogeneities or any other source of small gradients. We have selected the one-dimensional region on a central part of the LCLV, where illumination gradients and misalignment

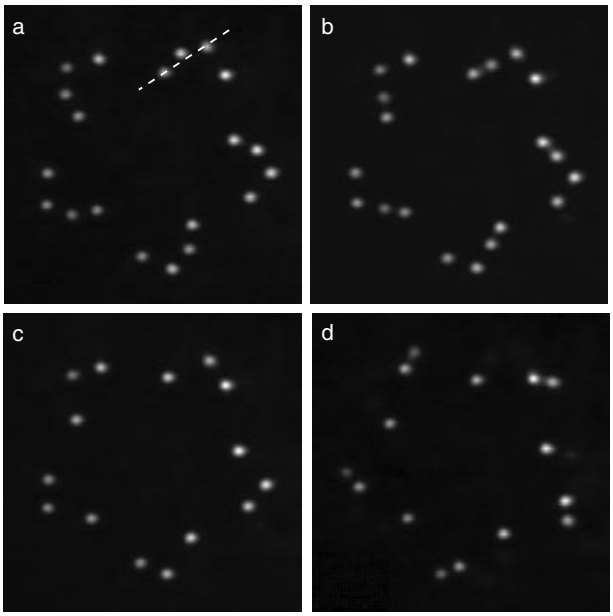

Figure 7. Instantaneous snapshots showing the oscillations of the localized structure positions. Times: (a) 0.0 s, (b) 2.6 s, (c) 5.0 s, (d) 8.2 s. The dashed line in (a) marks the one-dimensional cut along which the spatio-temporal diagram has been recorded.

Figure 8. Space (vertical)–time (horizontal) diagrams showing the periodic oscillations of the structure positions. The total elapsed time is 120 s.

effects are negligible. A rectangular mask is introduced in the optical feedback loop, just in contact with the entrance side of the fibre bundle. The width D of the aperture is 0.50 mm and its length l is 20 mm. The transverse aspect ratio $D/\Lambda \simeq 1$ is small enough for the system to be considered as one-dimensional, whereas the longitudinal aspect ratio $l/\Lambda \simeq 60$ is large enough for the system to be considered as a spatially extended one.

In figure 9 the instantaneous snapshots of three adjacent localized structures are shown, with two of them bouncing periodically in time one over the other. The corresponding spatial profiles are plotted in figure 10 whereas in figure 11(b) the corresponding spatio-temporal plot is displayed. In addition, figure 11(a) represents two stationary localized structures, whose position remains fixed during time, and figure 11(c) is the spatio-temporal diagram corresponding to the aperiodic oscillations in the positions of two adjacent localized structure.

6. Theoretical description

A one-dimensional model can be set up for the LCLV system, starting from the standard description of the optical feedback loop [12]. The light intensity I_{w} reaching the photoconductor is given by

$$I_{\mathrm{w}} = \frac{I_{\mathrm{in}}}{2}|\mathrm{e}^{\mathrm{i}\frac{L}{2k}\partial_{xx}}(1+\mathrm{e}^{-\mathrm{i}\beta\cos^2\theta})|^2$$

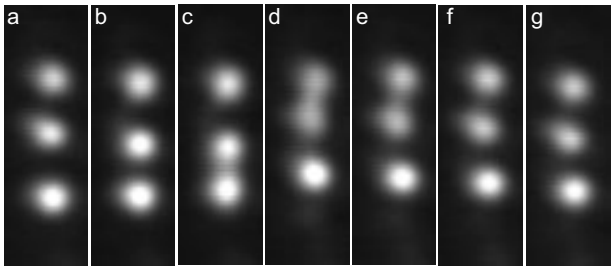

Figure 9. Instantaneous snapshots showing three bouncing localized structures. Times: (a) 0.0 s, (b) 1.0 s, (c) 1.3 s, (d) 1.7 s, (e) 2.1 s, (f) 2.4 s and (g) 2.8 s.

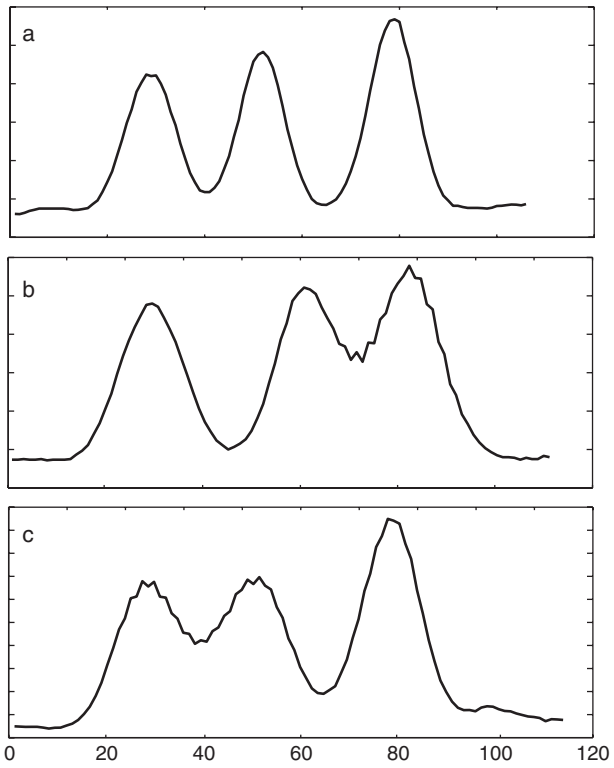

Figure 10. The spatial profile of the localized structures. Times: (a) 0.0 s, (b) 1.3 s and (c) 1.7 s. The horizontal scale is in pixel units.

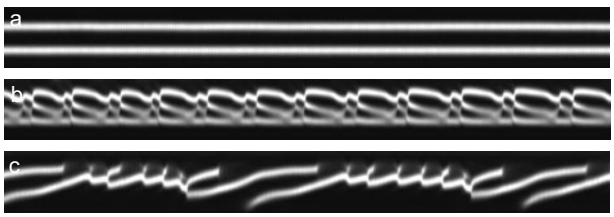

Figure 11. Space (vertical)–time (horizontal) diagrams showing (a) two stationary localized structures, (b) the periodic and (c) the aperiodic oscillations of the structure positions. The total elapsed time is 94 s.

where x is the transverse direction of the liquid crystal layer, and $\beta\cos^2\theta$ is the overall phase shift experienced by the light travelling forth and back through the liquid crystal layer; $\theta(x,t)$ is the average director tilt; $\beta = 2kd\Delta n$, where $k = 2\pi/\lambda$ is the optical wavenumber ($\lambda = 633$ nm), $d = 15$ μm is the thickness of the liquid crystal layer and $\Delta n = 0.2$ is the

difference between the extraordinary ($\parallel$ to $\vec{n}$) and ordinary ($\perp$ to $\vec{n}$) index of refraction of the liquid crystal.

In the absence of light on the photoconductor, the effective electric field $E_{\rm eff}$ applied to the liquid crystal layer is $E_{{\rm eff}\,(I_{\rm w}=0)} = \Gamma E_0 = \Gamma V_0/d$, where V_0 is the total voltage applied to the LCLV, and $\Gamma < 1$ is a transfer factor that depends on the electrical characteristics of the photoconductor, dielectric mirror and liquid crystal layers (impedances). As long as the light intensity is sufficiently small, that is, of the order of a few mW cm^{-2}, the response of the photoconductor can be fitted by a linear function. Under this approximation, the total effective electric field applied to the liquid crystal film can be expressed as $E_{\rm eff} = E_{{\rm eff}\,(I_{\rm w}=0)} + \alpha I_{\rm w}$, where α is a phenomenological dimensional parameter that can be quantitatively evaluated by fitting the open-loop response of the LCLV [35, 36].

$\theta = 0$ is the initial unperturbed planar alignment, whereas $\theta = \pi/2$ is the homeotropic alignment corresponding to the saturation of the molecular reorientation. The liquid crystal dynamics is described by a local relaxation equation of the form

$$\tau\partial_t\theta = l^2\partial_{xx}\theta - \theta + \frac{\pi}{2}\left(1 - \sqrt{\frac{V_{\rm FT}}{\Gamma V_0 + \alpha I_{\rm w}(\theta, \partial_x)}}\right) \qquad (1)$$

with $V \equiv \Gamma V_0 + \alpha I_{\rm w}(\theta, \partial_x) > V_{\rm FT}$, where $V_{\rm FT}$ is the Fréedericksz transition threshold voltage and l is the electric coherence length. It is important to remark that the above model have been deduced by fitting the experimental data measured for the open loop response of the LCLV [36], and it is slightly different with respect to the one proposed in [12].

The homogeneous equilibrium solutions are $\theta_0 = 0$ when $V \leqslant V_{\rm FT}$ and $\theta_0 = \pi/2\left(1 - \sqrt{V_{\rm FT}/V}\right)$ when $V > V_{\rm FT}$. Above the Fréedericksz transition, if we neglect the spatial terms, that is, for homogeneous equilibrium solutions, we find a closed expression for θ_0. Thus, disregarding diffraction, the light intensity reaching the photoconductor is

$$I_{\rm w} = \frac{I_{\rm in}}{2}|(1 + {\rm e}^{-{\rm i}\beta\cos^2\theta})|^2 = I_{\rm in}[1 + \cos(\beta\cos^2\theta)]$$

and

$$\theta_0 = \pi/2\left(1 - \sqrt{V_{\rm FT}/(\Gamma V_0 + \alpha I_{\rm in}[1 + \cos(\beta\cos^2\theta_0)])}\right).$$

The value of $V_{\rm FT}$ is set to $V_{\rm FT} = 3.2\ {\rm V_{rms}}$ in agreement with the experimental data for the LCLV system [35, 36]. The graph of $\theta_0(V_0, I_{\rm in})$ is plotted in figure 12. Several successive branches of bistability can be distinguished, corresponding to the critical points where $\theta_0(V_0, I_{\rm in})$ is a multi-valued function. Note that once the reorientation takes place, that is, $\theta_0 \neq 0$, the system looses the inversion symmetry around the equilibrium solutions.

Close to a point of nascent bistability, and neglecting the spatial derivatives, we can develop $\theta = \theta_0 + u + \cdots$ and derive a normal form equation

$$\partial_t u = \eta + \mu u - u^3 + {\rm h.o.t} \qquad (2)$$

where μ is the bifurcation parameter and η accounts for the asymmetry between the two homogeneous states. The higher order terms are ruled out by the scaling analysis, since

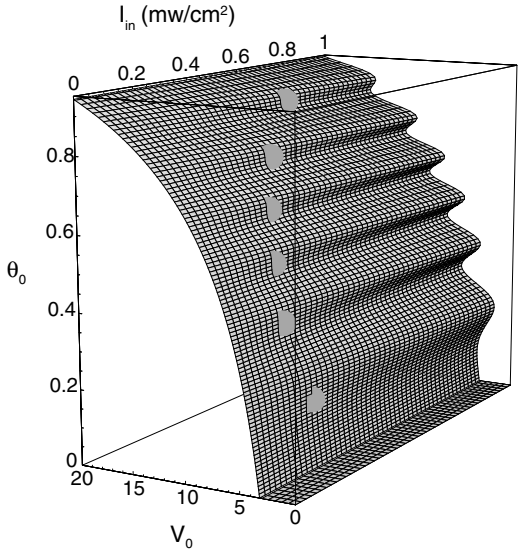

Figure 12. The multi-valued function $\theta_0(V_0, I_{\rm in})$. Shaded areas show the locations of the nascent bistability.

$u \sim \mu^{1/2}$, $\eta \sim \mu^{3/2}$ and $\partial_t \sim \mu$, $\mu \ll 1$. If we now consider the spatial effects, due to the elasticity of the liquid crystal and to the light diffraction, the system exhibits a spatial instability as a function of the diffraction length. Moreover, the spatial dependence of $I_{\rm w}$ is nonlocal, hence the dynamics of the above model, equation (1), is of non-variational type; that is, the system cannot be described by a Lyapunov functional.

The confluence of the nascent bistability and the spatial bifurcation gives rise to a multicritical point of co-dimension three. Close to this point, we derive an amplitude equation, that we call the Lifshitz normal form [29]:

$$\partial_t u = \eta + \mu u - u^3 + \nu\partial_{xx}u - \partial_{xxxx}u + du\,\partial_{xx}u + c(\partial_x u)^2 \quad (3)$$

where $\partial_x \sim \mu^{1/4}$, $\nu \sim \mu^{1/2}$ accounts for the intrinsic length of the system, $d \sim {\rm O}(1)$ and $c \sim {\rm O}(1)$. The term $\partial_{xxxx}u$ is a kind of super-diffusion, accounting for the short distance repulsive interaction, whereas the terms proportional to d and c are, respectively, the nonlinear diffusion and convection. When $\eta = d = c = 0$, the Lifshitz equation, equation (3), reduces to the generalized Swift–Hohenberg equation, that is well-known to describe pattern formation for many variational systems, such as in optics [27], chemistry [28] and liquid crystals [45]. Note that in optics, as a consequence of the phase invariance of the electric field amplitude, $d = c = 0$ is the most common situation, whereas $\eta \neq 0$ is a parameter proportional to the externally applied pump [27].

The model shows bistability between a homogeneous and a spatially periodic solutions and therefore it exhibits a family of localized structures. Depending on the choice of the parameters, localized structures may show periodic or aperiodic oscillations of their position, as confirmed by numerical simulations [34]. The full and lengthy derivation of the coefficients for the LCLV system is outside the scope of this article and will be reported elsewhere [44].

7. Conclusions

In the LCLV experiment, we have singled out a regime of parameters where the response of the LCLV is closely similar to that of a binary phase slice showing a point of nascent bistability. In these conditions, and by changing the feedback rotation angle $\Delta = 2\pi/N$, we are able to control the appearance of N-ordered configurations of localized structures, that can be seen as the spectral components of a crystal-like or a quasi-crystal-like structure function. By introducing a small non-local shift in the feedback loop, a dynamical motion of the localized structures over concentric rings is induced. All these manipulations can be exploited for applications in the field of optical computing and pattern recognition [40].

We have shown that, as soon as the input light intensity is slightly increased above the point of nascent bistability, the localized states show complex behaviour, such as periodic or aperiodic oscillations of their positions. We have related the intrinsic dynamics of the localized structures to the non-variational character of the LCLV system and we have derived a model taking it into account. The model is a Lifshitz normal form equation, that could in general be applied to a large class of different physical systems, the main requirements being the bistability and the presence of an intrinsic length (the diffraction length in the case of optics). Thus, we expect the observed dynamics to be quite general not only for an optical feedback system but also for other pattern forming systems.

Acknowledgments

We gratefully thank René Rojas for his help in calculations. M G Clerc acknowledges the support of Programa de inserción de científicos Chilenos of Fundación Andes, FONDECYT project 1020782, and FONDAP grant 11980002.

References

[1] Nicolis G and Prigogine I 1977 *Self-Organization in Non Equilibrium Systems* (New York: Wiley)
[2] For a review on pattern formation see, for example, Cross M and Hohenberg P 1993 *Rev. Mod. Phys.* **65** 581
[3] Fauve S and Thoual O 1990 *Phys. Rev. Lett.* **64** 282
[4] Eschenfelder H A 1981 *Magnetic Bubble Technology* (Berlin: Springer)
[5] Pirkl S, Ribiere P and Oswald P 1993 *Liq. Cryst.* **13** 413
[6] Astrov Y A and Logvin Y A 1997 *Phys. Rev. Lett.* **79** 2983
[7] Lee K-J, McCormick W D, Pearson J E and Swinney H L 1994 *Nature* **369** 215
[8] Lioubashevski O, Arbell H and Fineberg J 1996 *Phys. Rev. Lett.* **76** 3959
Lioubashevski O, Hamiel Y, Agnon A, Reches Z and Fineberg J 1999 *Phys. Rev. Lett.* **83** 3959
[9] Umbanhowar P B, Melo F and Swinney H L 1996 *Nature* **382** 793
[10] Lerman K, Bodenschatz E, Cannell D S and Ahlers G 1993 *Phys. Rev. Lett.* **70** 3572
[11] Mc Laughlin D W, Moloney J V and Newell A C 1983 *Phys. Rev. Lett.* **51** 75
[12] Neubecker R, Oppo G L, Thuering B and Tschudi T 1995 *Phys. Rev.* A **52** 791
[13] Ramazza P L, Ducci S, Boccaletti S and Arecchi F T 2000 *J. Opt. B: Quantum Semiclass. Opt.* **2** 399
[14] Iino Y and Davis P 2000 *J. Appl. Phys.* **87** 8251
[15] Ramazza P L, Benkler E, Bortolozzo U, Boccaletti S, Ducci S and Arecchi F T 2002 *Phys. Rev.* E **65** 066204
[16] Residori S, Nagaya T and Petrossian A 2003 *Europhys. Lett.* **63** 531
[17] Schaepers B, Feldmann M, Ackemann T and Lange W 2000 *Phys. Rev. Lett.* **85** 748
[18] Barland S *et al* 2002 *Nature* **419** 699
[19] See, for example, Coullet P 2002 *Int. J. Bifurcation Chaos* **12** 2445 and references therein
[20] McDonald G S and Firth W J 1993 *J. Opt. Soc. Am.* B **10** 1081
[21] Tlidi M, Mandel P and Lefever R 1994 *Phys. Rev. Lett.* **73** 640
[22] Brambilla M, Lugiato L A and Stefani M 1996 *Europhys. Lett.* **34** 109
[23] Firth W and Scroggie A J 1996 *Phys. Rev. Lett.* **76** 1623
[24] Saffman M, Montgomery D and Anderson D Z 1994 *Opt. Lett.* **19** 518
[25] Taranenko V B, Staliunas K and Weiss C O 1997 *Phys. Rev.* A **56** 1582
[26] Schaepers B, Feldmann M, Ackemann T and Lange W 2000 *Phys. Rev. Lett.* **85** 748
[27] Tlidi M, Mandel P and Lefever R 1994 *Phys. Rev. Lett.* **73** 640
[28] Hilali M F, Metens S, Borckmans P and Dewel G 1995 *Phys. Rev.* E **51** 2046
[29] Clerc M G 2003 *Phys. Lett.* A submitted
[30] Kuramoto Y 1984 *Chemical Oscillations, Waves and Turbulence* (Berlin: Springer)
[31] Coullet P, Lega J, Houchmanzadeh B and Lajzerowicz L 1990 *Phys. Rev. Lett.* **65** 640
[32] Kawagishi T, Mizuguchi T and Sano M 1995 *Phys. Rev. Lett.* **75** 3768
[33] Murray J D 1993 *Mathematical Biology* (Berlin: Springer)
[34] Clerc M G, Petrossian A and Residori S 2003 *Phys. Rev. Lett.* submitted
[35] Clerc M G, Residori S and Riera C S 2001 *Phys. Rev.* E **63** 060701(R)
[36] Clerc M G, Nagaya T, Petrossian A, Residori S and Riera C S 2004 *Eur. Phys. J.* D **28** 435
[37] Akhmanov S A, Vorontsov M A and Ivanov V Yu 1988 *JETP Lett.* **47** 707
Vorontsov M A and Miller W B 1995 *Self-Organization in Optical Systems and Applications in Information Technology* ed M A Vorontsov and W B Miller (Berlin: Springer)
[38] Arecchi F T, Boccaletti S, Ducci S, Pampaloni E, Ramazza P L and Residori S 2000 *J. Nonlinear Opt. Phys. Mater.* **9** 183
[39] Coullet P, Riera C and Tresser C 2000 *Phys. Rev. Lett.* **84** 3069
[40] Hayasaki H, Yamamoto H and Nishida N 2003 *Opt. Lett.* **28** 2351
[41] D'Alessandro G and Firth W J 1992 *Phys. Rev.* A **46** 537
[42] Pampaloni E, Ramazza P L, Residori S and Arecchi F T 1995 *Phys. Rev. Lett.* **74** 259
[43] Samson B A and Vorontsov M A 1997 *Phys. Rev.* A **56** 1621
[44] Clerc M G, Rojas R, Petrossian A and Residori S 2003 *Preprint* INLN 2003/10
[45] Michelson A 1977 *Phys. Rev. Lett.* **39** 464